REPORT DOCUMENTATION PAGE

Form Approved OMB No. 074-0188

1. AGENCY USE ONLY (Leave blank)	2. REPORT DATE	3. REPORT TYPE AND DATES COVERED
	April 1996	Scientific paper presented April 1996

4. TITLE AND SUBTITLE

Analysis of Advanced Oxidation Processes in a Hybrid Air Pollution Control System, 1996

5. FUNDING NUMBERS

N/A

6. AUTHOR(S)

B.A. Striebig, J.M. Schneider, T.A. Spaeder, M.R. Mallery, R.J. Heinsohn, & F.S. Cannon

7. PERFORMING ORGANIZATION NAME(S) AND ADDRESS(ES)

The Applied Research Laboratory
The Pennsylvania State University
State College, PA 16804

8. PERFORMING ORGANIZATION REPORT NUMBER

N/A

9. SPONSORING / MONITORING AGENCY NAME(S) AND ADDRESS(ES)

SERDP
901 North Stuart St. Suite 303
Arlington, VA 22203

10. SPONSORING / MONITORING AGENCY REPORT NUMBER

N/A

11. SUPPLEMENTARY NOTES

Presented at the International Chemical Oxidation Association's 6th Annual Symposium on Chemical Oxidation: Technology for the Nineties, Nashville, TN, April 1996. This work was supported in part by SERDP et al..

12a. DISTRIBUTION / AVAILABILITY STATEMENT

Approved for public release: distribution is unlimited

12b. DISTRIBUTION CODE

A

13. ABSTRACT ***(Maximum 200 Words)***

With the passage of the 1990 Clean Air Act, advanced oxidation processes have gained interest as an alternative for treating a variety of industrial air and waster water streams. These advanced oxidation processes are very attractive when contaminant compositions and concentrations in the air stream vary widely making typical catalytic incineration costly in terms of fuel and potential catalyst fouling. SERDP and the Marine Corps. Logistics Base have sponsored research on a 2600 scfm pilot scale hybrid air treatment system at The Applied Research Laboratory, The Pennsylvania State University.

14. SUBJECT TERMS

SERDP, Oxidation, Waste treatment

15. NUMBER OF PAGES

26

16. PRICE CODE N/A

17. SECURITY CLASSIFICATION OF REPORT	18. SECURITY CLASSIFICATION OF THIS PAGE	19. SECURITY CLASSIFICATION OF ABSTRACT	20. LIMITATION OF ABSTRACT
unclass.	unclass.	unclass.	UL

Striefig, B.A., J. Dusenbury, R.J. Heinsohn, M. Mallery, J.M. Schneider and T. Spaeder. *"Analysis of Advanced Oxidation Processes in a Hybrid Air Pollution Control System."* Presented at the Internation Chemical Oxidation Association's 6th Annual Symposium on Chemical Oxidation: Technology for the Nineties, Nashville, TN, April 1996.

Title: Analysis of Advanced Oxidation Processes in a Hybrid Air Pollution Control System, 1996

Authors: Bradley A. Striebig
J. M. Schneider
T. A. Spaeder
M. R. Mallery
R. J. Heinsohn
F. S. Cannon

Bradley A. Striebig
The Applied Research Laboratory
The Pennsylvania State University
P. O. Box 30
State College PA, 16804

ABSTRACT

With the passage of the 1990 Clean Air Act, advanced oxidation processes have gained interest as an alternative for treating a variety of industrial air and waste water streams. These advanced oxidation processes are very attractive when contaminant compositions and concentrations in the air stream vary widely making typical catalytic incineration devices costly in terms of fuel and potential catalyst fouling. The Strategic Environmental Research and Development Program (SERDP) and the Marine Corps. Logistics Base (MCLB) have sponsored research on a 2600 scfm pilot scale hybrid air treatment system at The Applied Research Laboratory, The Pennsylvania State University.

The hybrid system has been used at the pilot scale and commercial level to remove a variety of volatile organic compounds from exhaust air streams. The pilot scale system has been operated for more than 100 hours at The Applied Research Laboratory from December, 1994 to January, 1996. The results of bench scale experimentation, numerical modeling, and pilot scale evaluation were combined to describe the removal mechanisms and oxidative degradation of organic compounds. System performance was evaluated for solvents that are typically present in Marine Corps surface coatings, including alcohols, ketones, aromatic hydrocarbons, and chlorinated solvents. The active removal mechanism in the hybrid system was found to be related to the solvent's chemical functionality and physical attributes.

The pilot scale hybrid air pollution control technology was effective in removing volatile compounds from the exhaust air streams over 100 hours of operation. Addition of hydroxyl radical producing oxidants in the gas and aqueous phases, and optimization of the reactor design may significantly reduce the costs of the hybrid systems in future applications. The reactor components provided synergistic VOC treatment alternatives which can be operated at ambient temperatures using advanced oxidation processes.

INTRODUCTION

Volatile organic compounds (VOCs) make up a large group of chemicals used in many industrial processes, including surface coating, cleaning, and lubrication processes. The use of VOCs rose dramatically in the twentieth century. Industries required large quantities of chemicals to meet the demand for consumer goods. The use of VOCs increased the release of VOCs into the troposphere. VOCs in the troposphere react with nitrous oxides and form photochemical smog [1]. The passage of the 1990 Clean Air Amendments addressed environmental and health concerns associated with photochemical smog. The Clean Air Amendments set strict environmental regulations governing the use and the release of VOCs into the atmosphere.

The passage of the Clean Air Amendments encouraged the Marine Corps Logistics Base (MCLB) to investigate VOC abatement technologies at installations where surface coating operations were conducted. A system was required to treat 45,000 SCFM of exhaust air from a paint booth where Chemical Agent Resistant Coatings (CARC) were applied to vehicles and parts. The MCLB chose a hybrid air pollution control system (APCS) that had been designed by Terr-Aqua Environmental Systems (TAES) for a facility located at Barstow, CA.

Funds were allocated through the Strategic Environmental Research and Development Program (SERDP) to evaluate and improve the hybrid APCS designed for the Barstow Marine Corp. Logistics Base. The SERDP program was a joint research effort by the United States Environmental Protection Agency (USEPA) and MCLB, in conjunction with its research partner, The Applied Research Laboratory (ARL) at The Pennsylvania State University. The goal of the SERDP program was to effect a rapid improvement in the quality of air emissions at MCLBs by applying, evaluating, and improving innovative pollution prevention and control technology approaches. As part of the joint effort task force, ARL Penn State's responsibility was to perform modeling and experimentation to feed an iterative cycle of enhanced understanding of the [hybrid air pollution control system] processes, optimization of the field [air treatment] system, and additional data collection.

The APCS consisted of an ambient humidity ultra-violet (UV) reaction chamber, a mist air dispersion spray chamber, a packed column aqua-reactor, and a high humidity UV reaction chamber in series followed by two carbon sorption beds. Water from the APCS packed column chemical absorption reactor was sent to an ozonated water recycle tank. A schematic of the hybrid APCS is shown in Figure 1. Each individual unit process is described in detail in this paper.

Three separate reaction processes within the APCS were investigated by ARL Penn State. One group of researchers conducted analytical and experimental studies upon a simulated bench-scale UV reaction chamber of the APCS [2]. A second group studied mass transfer effects and optimization of advanced oxidation processes in the chemical absorption reactor and water recycle tank. Another group focused on the bench-scale carbon adsorption of VOCs and ozonation regeneration reactions [3,4].

This paper will present a scientific explanation of the important removal mechanisms within the hybrid air pollution control system. Each reactor unit is examined in a stepwise fashion as shown in Figure 1, starting with the photolytic reactors, the chemical-absorption reactors, and then the carbon bed. Modeling and bench-scale experimental data were

evaluated as well to suggest changes which may increase the removal efficiency and/or cost effectiveness of future systems. These bench-scale results are also reported before or after the pilot scale unit which they parallel.

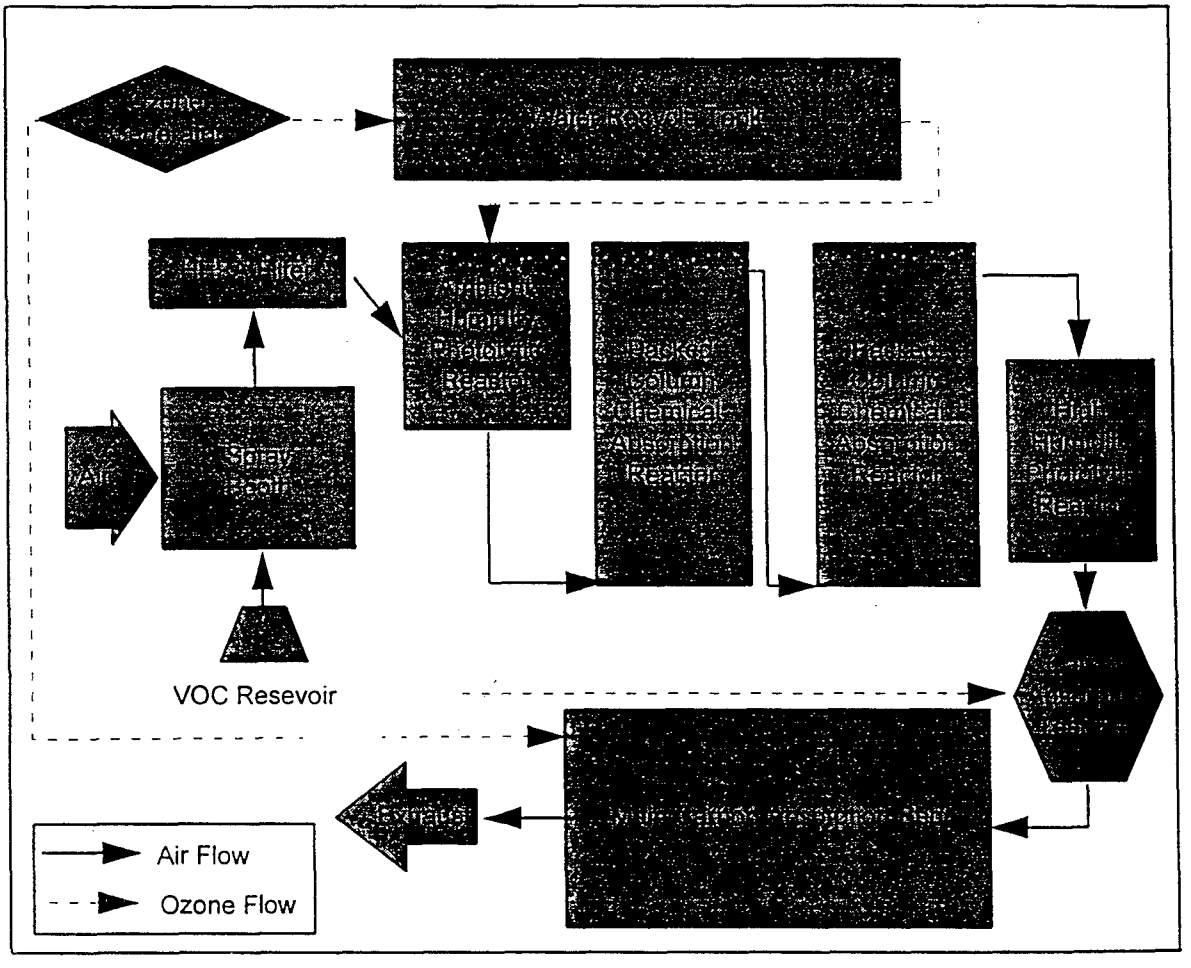

Figure 1: Schematic of the pilot scale air pollution control system

EQUIPMENT AND METHODS

PILOT SCALE SYSTEM

A pilot scale air treatment system was installed at The Applied Research Laboratory. The pilot scale system, designed to scale, represented air treatment systems currently in full-scale operation. Several modifications, however, were made so that investigators could examine changes in operating conditions. Thus far, modifications of the following parameters have been studied: number of UV bulbs contained in each photolytic reactor (3 to 7 bulbs), the volumetric flow rate of air to be treated (1300 cfm to 2600 cfm), operation of the mist air dispersion units (on or off), and pH control and hydrogen peroxide addition in the water recycle tank.

Air and water sampling ports were located within the system fore and aft of each unit. Bench scale and pilot scale air and water samples were analyzed by capillary gas chromatography using either flame ionization (FID), thermal conductivity (TCD), electron capture (ECD), or mass selective (MS) detectors. Air samples were typically analyzed with the aid of cryoconcentration and cryofocusing. Water samples were analyzed in the aqueous phase, diluted with an internal standard, or concentrated in a liquid-liquid extraction process. All samples were quantified using single point calibrations after linearity in the concentration range of interest had been validated.

The following general procedure was followed during pilot scale system experiments. A VOC was spayed into the incoming air stream to achieve an inlet concentration of approximately 100 ppm. This concentration was similar to those experienced in the Marine Corp. Logistics Base spray booths (0-300 ppm) [6]. Fluctuations in the actual air stream concentrations made it necessary to normalize some of the data contained within this report. Typical experimental run times were 2-12 hours, with periodic sampling throughout the system over this time. More than 100 hours of elapsed running time was logged on the pilot scale system. The chemical absorption reactors were significantly influenced by time, thus much of the sampling was concentrated around these units. Concentrations exiting the photolytic reactors and the virgin carbon bed changed very little with time.

The pilot scale chemical absorption reactor was modified based on bench-scale results. Phosphate buffers and sodium hydroxide were used to maintain a constant pH of 9 in the aqueous reactors and water recycle tank. Hydrogen peroxide was added in the chemical absorption reactor at 0.5 mole of hydrogen peroxide per mole of ozone absorbed to increase organic destruction based upon bench scale results. Pilot scale optimization of the chemical-absorption reactor columns was verified by analysis of a semi-polar organic compound (MEK).

BENCH SCALE SYSTEMS

Changes in the pilot scale and/or full-scale systems were evaluated first by modifying the bench scale reactors. The bench scale photolytic reactor and analytical models were used to simulate reactions which occurred in the presence of one or two UV radiation sources. The bench scale photolytic reactor and model variables evaluated included higher intensity UV sources, higher ozone concentrations and variable organic concentrations. Ozone concentrations, pH control, hydrogen peroxide addition, and lower flow rates were the primary parameters evaluated in the bench scale chemical absorption reactor.

The bench scale photolytic reactor consisted of a rectangular duct that contained a cylindrical lamp which emitted electromagnetic radiation in the ultraviolet light spectrum. The radiation source provided energy over the wavelength range of 238 to 579 nm (ultra-violet). The UV radiation source was the TQ718 (700W) medium pressure mercury arc lamp manufactured by Hereaus Amersil in Germany. The bench scale photolytic reactor was operated under steady state conditions. Thus, variables including the organic concentration and ozone concentration were evaluated individually at several different concentrations. "Light" and "dark" experiments were conducted to measure the effects of UV radiation upon the degradation of methanol. These variables were chosen based upon analytical evaluation of the chemical kinetics with the photolytic reactor analytical model.

The effects of advanced oxidation processes upon organic destruction in the aqueous phase were determined in a 1 liter constantly stirred (well-mixed) tank reactor (CSTR). A schematic of the CSTR is shown in Figure 2. Reagent grade N-methyl-2-pyrrolidinone (NMP) from Aldrich Chemical Co. was used. There were no mechanistic reactions found for the oxidation of NMP in the published literature. Data for the degradation of alcohols, ketones, and aromatics have been cited in the literature [5]. Experiments carried out in a constantly stirred tank reactor (CSTR) included measuring the relative effects of pH, ozone concentrations, and hydrogen peroxide concentrations on the degradation of NMP. Studies consisted of measuring the concentration of NMP and reaction products in the CSTR over time with the addition of ozone and hydrogen peroxide. Hydrogen peroxide from a 35% by weight stock solution was added to the CSTR at a constant flow rate. Ozone was generated by the Oxytech model PXC-20 ozone generator. Ozone concentrations were measured in the inlet and exhaust air streams with a Dasibi model 1008-HC ozone meter. Solutions were buffered with phosphate salts and the pH was adjusted with sodium hydroxide to maintain a constant pH. The pH and temperature of the system were monitored with an Orion ATP probe and model 250 Orion pH meter.

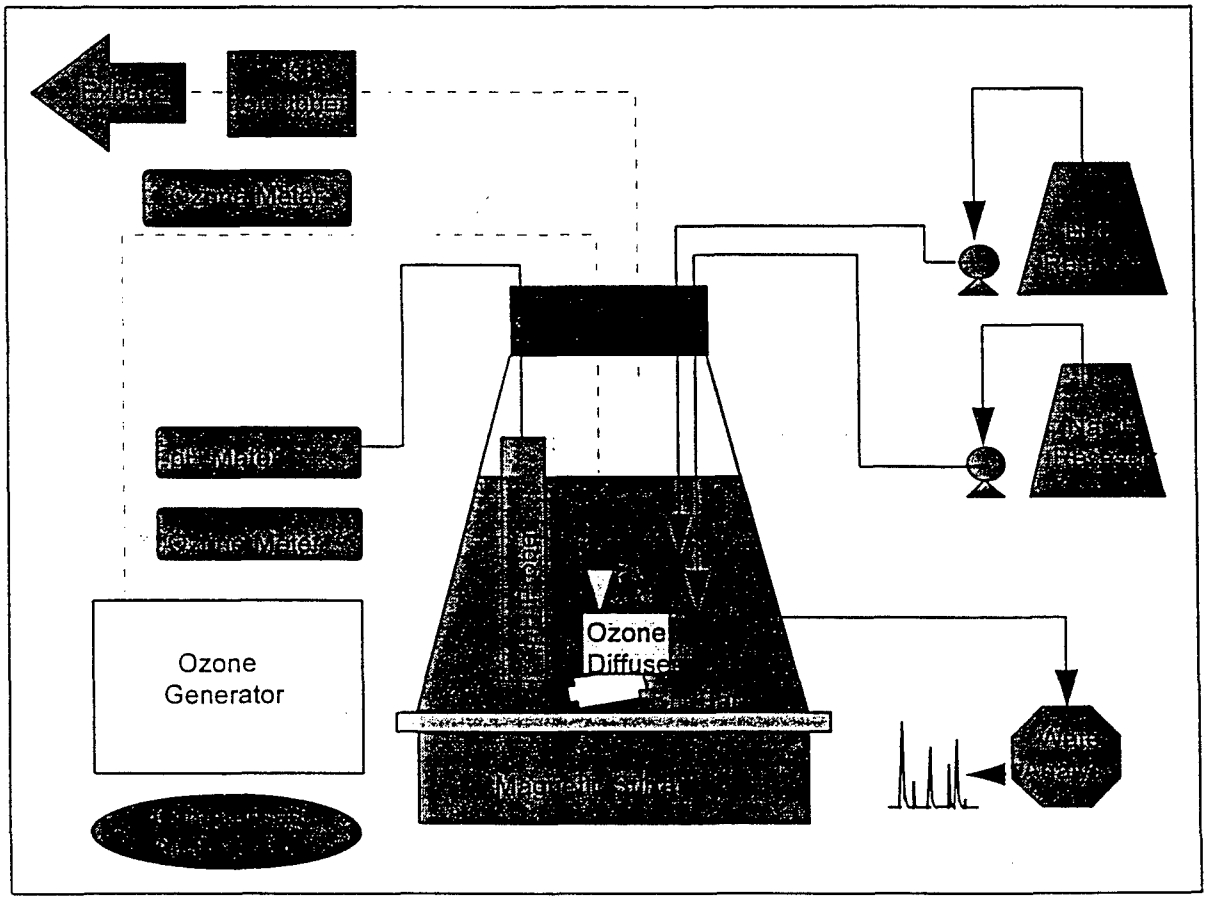

Figure 2: Schematic of the constantly stirred tank reactor (CSTR) for optimization of organic destruction by advanced oxidation processes.

Several solvents were evaluated at the pilot scale levels. Solvents were chosen to represent general classes of organic compounds representative of solvents found in surface coatings used by MCLB. Solvents investigated in the pilot scale system included ethanol, ethylbenzene, methylethyl ketone (MEK), and trichloroethylene (TCE) obtained from Aldrich Chemical Co. Reagent grade ethanol, methanol, methyl isobutyl ketone (MIBK), benzene, toluene, and tetrachloroethylene (PCE) were used in the evaluation of the GAC, as discussed elsewhere [3,4].

The durability and absorption capacity of the virgin carbon after continuous regeneration was of great interest, and could not be simulated in the pilot scale system over the short duration of the pilot scale evaluation. Thus, granular activated carbon was obtained from full-scale commercial sites that use the hybrid APCS described to treat exhaust air from a furniture coating manufacturer, an aircraft panel manufacturer, and aircraft coating manufacturer. Virgin carbon samples of GAC from two of these facilities was available for comparison. Pore structure characterization studies were conducted using the accelerated Surface Area and Posimetric System, ASAP 2000, from Micromeretics (Norcross, Ga.). The NIOSH method # 1003 was adapted to evaluate the VOC loading onto the GAC. This method is a carbon disulfide extraction process. The extract was then analyzed by capillary gas chromatography.

Findings for each individual reactor (photolytic reactors, chemical-absorption reactors, and carbon bed) are discussed individually below, followed by a summary which compares the complete system profiles for the four compounds tested in the pilot scale system.

RESULTS AND DISCUSSION

ANALYTICAL MODEL OF A PHOTOLYTIC REACTOR

A computational fluid dynamics (CFD) model has been developed which describes the interactions between the fluid dynamics of a volatile organic laden gas stream and the photochemical and chemical processes occurring within a photolytic reactor. The reactor model shown in Figure 3, consists of a rectangular duct containing two cylindrical lamps in series which emit electromagnetic radiation in the ultraviolet light spectrum. The radiation sources provide energy over the wavelength range of 238 to 579 nm (ultraviolet). The sources were modeled from manufacturers data on the TQ718 (700W) medium pressure mercury arc lamps manufactured by Hereaus Amersil in Germany. The fluid flow field in the reactor was modeled using Harwell (CFDS)-FLOW3D software, a Computational Fluid Dynamics (CFD) package developed by Harwell Laboratory in the United Kingdom.

The light intensity distribution within the reactor was modeled based upon the integrated form of the Beer-Lambert Law:

$$I_r = \frac{r_o I_{ro}}{r} e^{-(r-r_o)\sum[C]\sigma} \qquad (1)$$

It was assumed that radiation was emitted solely in the radial direction and that formaldehyde (HCHO) and ozone (O_3) were the only chemical species which contributed

significantly to light attenuation in the reactor. The photolytic rate constants for HCHO, O_3, and hydrogen peroxide (H_2O_2) were then calculated with equation (2) which takes into account the radial variation of light intensity:

$$k = \frac{r_o}{r}\sum_{\lambda_1}^{\lambda_n}\sigma(\lambda,T)\phi(\lambda,T)e^{-(r-r_o)\sum[C]\sigma}J(\lambda) \qquad (2)$$

where $\phi(\lambda,T)$ is the quantum yield of the reaction, $\sigma(\lambda,T)$ is the absorption cross-section of a given molecule, and $J(\lambda)$ is the actinic flux emitted by the light source. The photolytic rate constants are calculated by summing over discrete wavelengths. Twelve wavelengths over a range of from 248-366 nm were used in the equation to model the photolytic rate constants.

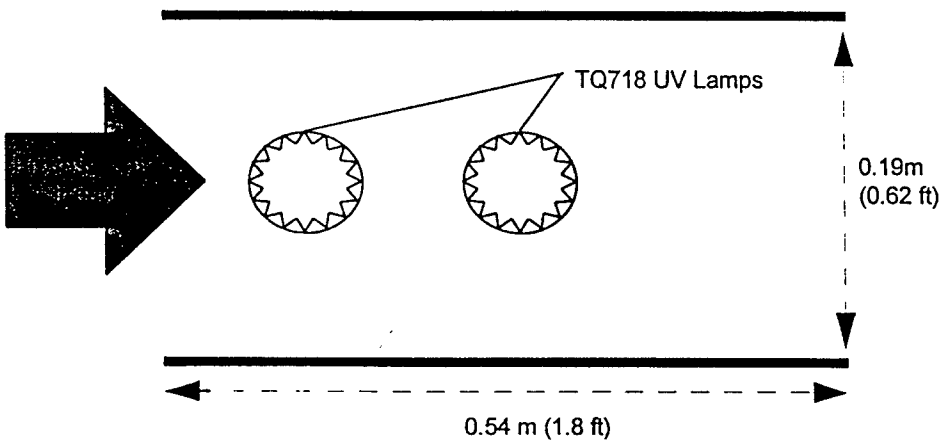

Figure 3: Analytical representation of the photolytic reactor

The photolytic rate constants were used in a reduced chemical kinetic model for the oxidation of HCHO in the presence of ultraviolet light and O_3. Twenty three chemical reactions involving 14 chemical species were analyzed in the model and are listed in Table I. These 14 species and 23 reactions were reduced from a set of 56 chemical reactions for 21 species compiled from the literature [7,8]. The reduced chemical equation set was essential for use in the flow field model to reduce computational time and costs. The reduced chemical kinetic model did not significantly differ from the full chemical kinetic model for residence times in a well mixed reactor of less than three seconds. The reduced chemical kinetics model was presumed valid, since residence times in the model and experimental reactors were less than three seconds.

The kinetic mechanisms which lead to generation or removal of a given species are incorporated as source/sink terms, symbolized by S, in the species mass conservation equation given below:

$$\rho\bar{u}_j\frac{\partial C}{\partial x_j} - \frac{\partial}{\partial x_j}\left(\left(\frac{\mu T}{\sigma_S} + \rho D\right)\frac{\partial C}{\partial x_j}\right) = S \qquad (3)$$

$$S = S_p + S_u \tag{4}$$

TABLE I - CHEMICAL REACTIONS INCORPORATED INTO FLOW FIELD MODEL OF REACTOR

Radical Oxidation Reactions Modeled	Rate Constant (cm^3/molecule)	Reference
$OH^{\bullet} + O_3 \rightarrow HO_2^{\bullet} + O_2$	6.8e-14	[9]
$HO_2^{\bullet} + O_3 \rightarrow OH^{\bullet} + 2O_2$	2.0e-15	[9]
$HCO^{\bullet} + O_2 \rightarrow HO_2^{\bullet} + CO$	5.5e-12	[9]
$OH^{\bullet} + OH^{\bullet} \rightarrow O(^1D) + H_2O$	1.9e-12	[9]
$OH^{\bullet} + HO_2^{\bullet} \rightarrow O_2 + H_2O$	1.1e-10	[9]
$OH^{\bullet} + H_2O_2 \rightarrow HO_2 + H_2O$	1.7e-12	[9]
$CO + OH^{\bullet} \rightarrow CO_2 + H^{\bullet}$	1.5e-12	[9]
$HCHO + OH^{\bullet} \rightarrow HCO^{\bullet} + H_2O$	1.0e-11	[9]
$H^{\bullet} + O_2 \xrightarrow{M} HO_2$	1.2e-12	[10]
$H^{\bullet} + O_3 \rightarrow OH + O_2$	2.9e-11	[9]
$HO_2^{\bullet} + HO_2^{\bullet} \rightarrow H_2O_2 + O_2$	1.6e-12	[9]
$CO + HO_2^{\bullet} \rightarrow CO_2 + OH^{\bullet}$	1.9e-32	[9]
$O(^1D) + N_2 \rightarrow O(^3P) + N_2$	2.6e-11	[9]
$O(^3P) + O_2 \xrightarrow{M} O_3$	1.0e-14	[9]
$O(^1D) + H_2O \rightarrow OH^{\bullet} + OH^{\bullet}$	2.2e-10	[9]
$O(^1D) + O_2 \rightarrow O(^3P) + O_2$	4.0e-11	[9]
$CH_3OH + OH^{\bullet} \rightarrow CH_2OH + H_2O$	7.8e-13	[11]
$CH_3OH + OH^{\bullet} \rightarrow CH_3O + H_2O$	1.4e-13	[11]

Photolytic Reactions Modeled	Rate Constant at the Bulb Surface (seconds $^{-1}$)	Reference
$HCHO + h\nu \rightarrow H^{\bullet} + HCO^{\bullet}$	0.0091	[12]
$HCHO + h\nu \rightarrow H_2 + CO$	0.0033	[12]
$O_3 + h\nu \rightarrow O_2 + O(^1D)^{\bullet}$	1.900	[11]
$O_3 + h\nu \rightarrow O_2 + O(^3P)^{\bullet}$	0.2150	[11]
$H_2O_2 + h\nu \rightarrow OH^{\bullet} + OH^{\bullet}$	0.0133	[11]

This equation includes advection, diffusion and chemical transformation for a given chemical species. To account for the chemical reaction kinetics in each scalar equation, the source term is linearized into two components: S_p and S_u. S_p includes all source terms which contain the dependent variable and act as a sink for that variable. S_u contains all other source

terms including those terms which act as a source for the dependent variable. The mass conservation equations were applied to the following species: HCHO, CH_3OH, OH•, H•, HO_2•, $O(^3P)$, $O(^1D)$, H_2O_2, O_3, HCO, and CO.

Time averaged velocity distributions are calculated in the reactor using the Reynolds Averaged Navier-Stokes (RANS) form of the momentum equation and the mass conservation equation. A two-equation k-ε turbulence model with incompressible Newtonian flow is also assumed with this model. The photolytic reactor geometry provided in Figure 3 was modeled with a two dimensional body fitted grid containing 136 nodes in the flow wise direction and 24 nodes in the cross-wise direction. Low concentration levels for the eleven species calculated in the model allow the momentum and species conservation equations to be decoupled. This leads to a simplification of the solution methods for this problem which are pressure based.

The equation set modeled is provided below. The final model includes the numerical solution of 16 equations for the following 16 unknowns: x-velocity (u_1), y-velocity (u_2), pressure (p), turbulent kinetic energy dissipation rate (ε), turbulent kinetic energy (k) and 11 chemical species concentrations. The temperature variation within the reactor induced by radiant energy emitted by the TQ718 lamp was not modeled at this time.

Mass Conservation:

$$\frac{\partial u_i}{\partial x_i} = 0 \tag{5}$$

Effective Viscosity:

$$\mu_{eff} = \mu + \mu_T = \mu + C_\mu \rho \frac{k^2}{\varepsilon} \tag{6}$$

RANS equation:

$$\rho \bar{u}_j \frac{\partial \bar{u}_i}{\partial x_j} = -\frac{\partial p \delta_{ij}}{\partial x_j} + \frac{\partial}{\partial x_j}(\mu_{eff}(\frac{\partial \bar{u}_i}{\partial x_j} + \frac{\partial \bar{u}_j}{\partial x_i})) \tag{7}$$

k-equation:

$$\rho \overline{u_j} \frac{\partial k}{\partial x_j} = \frac{\partial}{\partial x_j}((\mu + \frac{\mu_T}{\sigma k})\frac{\partial k}{\partial x_j}) - \rho\varepsilon + \mu_{eff}\frac{\partial \bar{u}_i}{\partial x_j}(\frac{\partial \bar{u}_i}{\partial x_j} + \frac{\partial \bar{u}_j}{\partial x_i}) \tag{8}$$

ε- *equation:*

$$\rho \overline{u_j} \frac{\partial \varepsilon}{\partial x_j} = \frac{\partial}{\partial x_j}((\mu + \frac{\mu_T}{\sigma_\varepsilon})\frac{\partial \varepsilon}{\partial x_j}) - \rho C_2 \frac{\varepsilon^2}{k} + C_1 \frac{\varepsilon}{k}\mu_{eff}\frac{\partial \bar{u}_i}{\partial x_j}(\frac{\partial \bar{u}_i}{\partial x_j} + \frac{\partial \bar{u}_j}{\partial x_i}) \tag{9}$$

ANALYTICAL MODEL RESULTS OF THE PHOTOLYTIC REACTOR

Parametric modeling studies were performed which varied the strength of the ultraviolet energy source and the inlet ozone concentration. The analytical model predicted that direct photolysis of HCHO was an order of magnitude slower than destruction of HCHO by hydroxyl radical attack. By increasing the ozone concentration, the production of the hydroxyl radicals from the reactions in Table 1 was increased. Thus, the destruction of HCHO increased with increasing inlet O_3 concentrations. This is illustrated in Figure 4 which shows the HCHO concentration contours throughout the reactor for an inlet HCHO concentration of 1000 ppm and inlet ozone concentrations of 300 ppm and 75 ppm respectively. When the inlet ozone concentration was 75 ppm, the analytical model predicted that HCHO reduction was confined to the bulb wake regions and was limited to 5% (50 ppm). The predicted HCHO concentration with an inlet ozone concentration of 100 ppm, on the other hand, decreased below 850 ppm, or 15% reduction in the wake region behind each bulb. The average reduction throughout the reactor for the high ozone condition was approximately 4%, whereas an inlet ozone concentration of 75 ppm only resulted in an average of 2% destruction.

The light intensity which was transmitted through the reactor was dependent upon the concentration of chemical species in the reactor and their respective absorption cross-sections. Based on equation 2, the model predicts that the light intensity drops off rapidly with increasing distance from the bulb. At two bulb diameters downstream of the second bulb, less than 10% of the light was transmitted. Figure 5, shows the corresponding decrease in HCHO degradation with increasing distance from the UV source for the nominal light intensity case and for a 10-fold increase in light intensity. A significant increase in HCHO degradation was predicted with a 10 fold increase in light intensity. An average HCHO destruction rate predicted across the outlet of the reactor was 14% for the 10-fold increase in light intensity compared to 1% for nominal light intensity conditions.

Significant interactions between the fluid flow field and chemical reactions were observed. High rates of degradation were seen in the wake regions of the UV bulbs, as shown in Figures 4 and 5. It is proposed that the bulb wake regions allowed more contact time between the hydroxyl radical and HCHO which resulted in higher degradation rates. Based on the results of this modeling study, the photolytic reactor should have the bulbs arranged as closely as possible. The close arrangement should optimize the light intensity and recirculation regions of the process stream within the reactor which influence organic degradation.

BENCH SCALE PHOTOLYTIC REACTOR RESULTS

Experimental studies were conducted in a bench scale photolytic reactor. These studies were designed to verify that the ozone concentration and ultraviolet radiation had a significant impact upon the degradation of methanol in the bench scale photolytic reactor. These studies were compared qualitatively to the prediction of the analytical model.

The data presented in Figure 6 shows that more methanol was oxidized at higher ozone concentrations than at low ozone concentrations, as predicted by the analytical model. Degradation of methanol was also enhanced by ultraviolet radiation. This enhancement was also predicted by the analytical model. However, significant degradation induced by "dark"

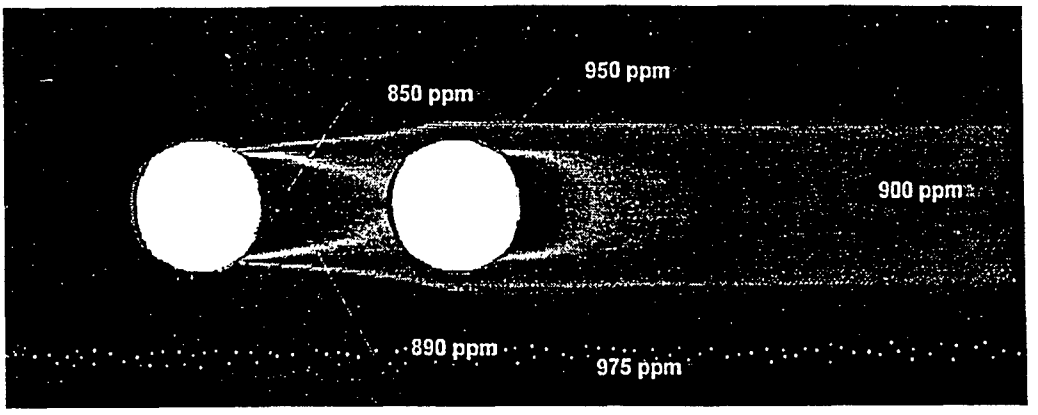

Ozone Inlet Concentration of 300 ppm, Air Stream Inlet Velocity of 0.5 m/s

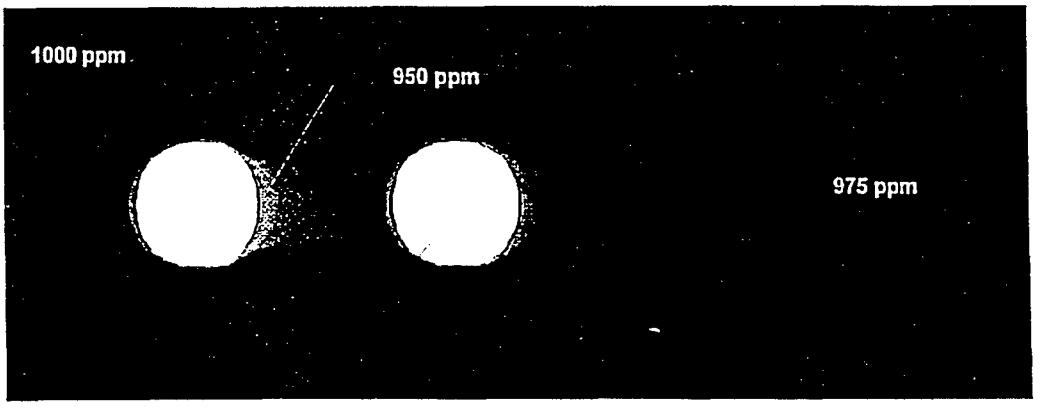

Ozone Inlet Concentration of 75 ppm, Air Stream Inlet Velocity 0.5 m/s

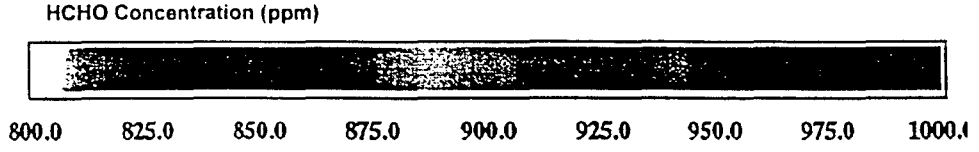

Figure 4 Effect of inlet ozone concentration on HCHO removal in the reactor.

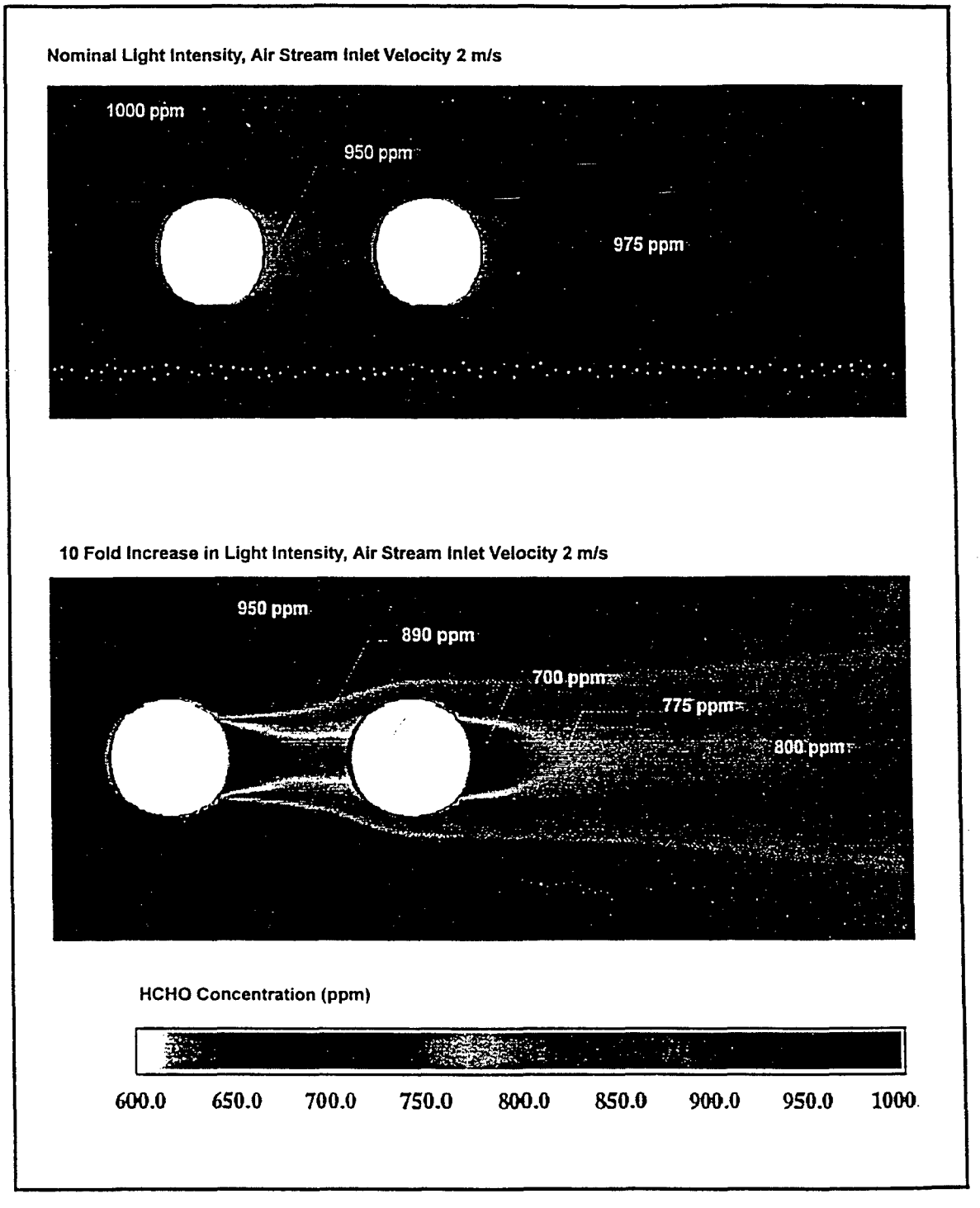

Figure 5: Effect of light intensity on HCHO destruction in the reactor.

reactions did occur in the reactor in the absence of the UV radiation which was not predicted by the analytical model.

One possible explanation of why the analytical model did not predict these "dark" reactions was that the direct ozonation reactions of methanol with ozone were not included in the analytical model. The direct ozonation of methanol in the gas phase was not included because the reported reaction rate of methanol with ozone is over eight orders of magnitude less than the reaction rate with the hydroxyl radical [13,14]. Furthermore, reaction rate constants for ozone and methanol in the gas phase were not found in the literature. Therefore, prior to the bench scale results, the direct ozonation of methanol in the air phase was considered insignificant.

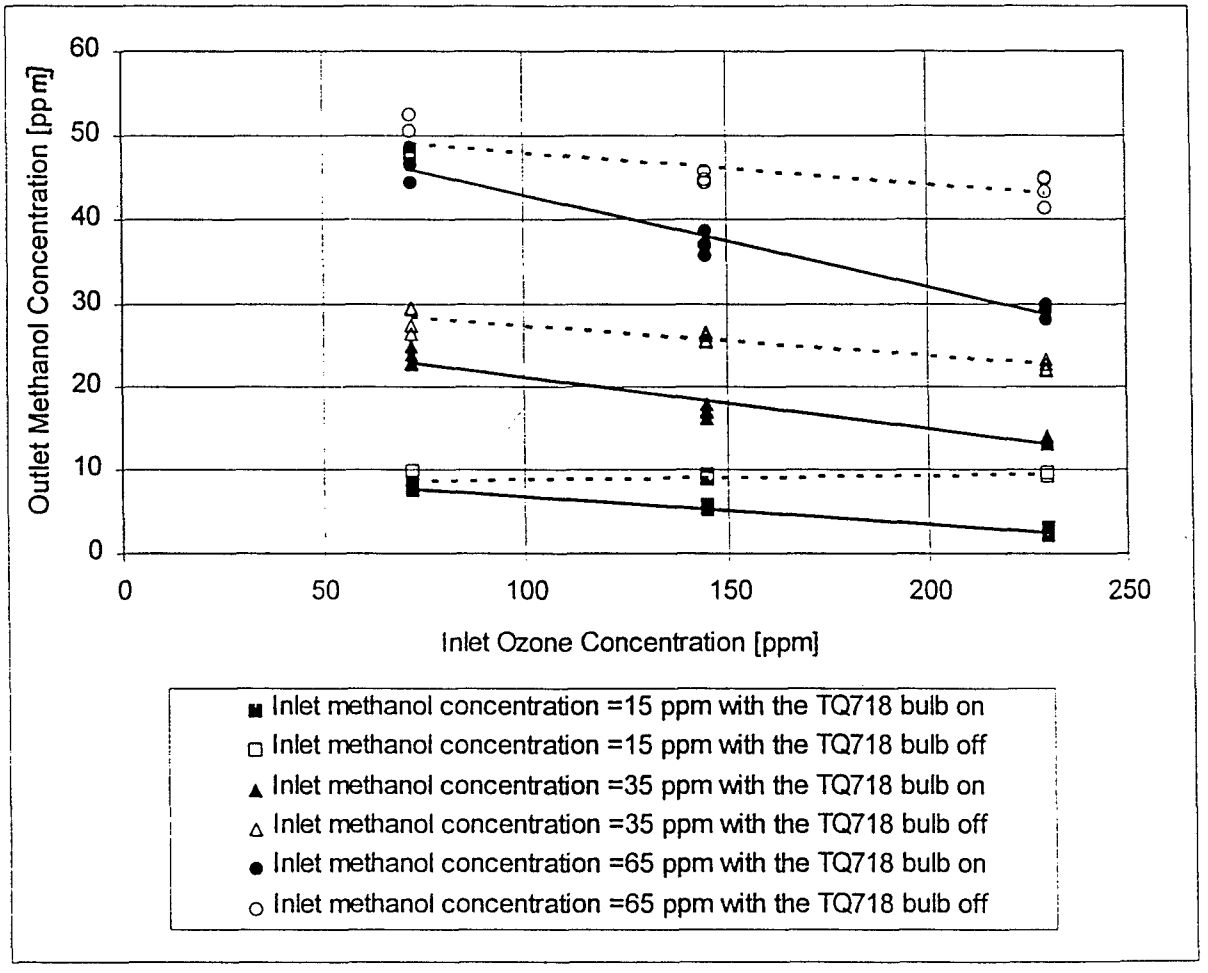

Figure 6: Effects of ozone concentration and ultraviolet radiation upon the degradation of methanol in a bench-scale photolytic reactor

However, in light of the experimental results, it is proposed that direct ozonation may be a significant contributor to methanol degradation in the bench-scale photolytic reactor. The analytical model predicts that the maximum OH radical concentration near a UV source is less than 1 ppb. Furthermore, the OH radical concentration throughout the domain of the

entire reactor was predicted to be much less than 1 ppb. Ozone concentrations within the bench scale reactor were on the order of 100 ppm. Thus the ozone concentration within the reactor was at least five orders of magnitude greater than the OH radical concentration. Thus even though the reaction rate of methanol and ozone is much smaller than the reaction rate with the hydroxyl radical, it may be a significant reaction mechanism because the ozone concentration is much greater across the entire domain of the reactor than the OH radical concentration. New modeling techniques are currently being developed to account for the ozone and methanol reactions.

The analytical and experimental results indicate that organics can be oxidized in a gas-phase photolytic reactor. The addition of ozone to the photolytic reactor significantly enhanced organic destruction. Increased light intensity also increased photolytic destruction of organic compounds.

PHOTOLYTIC REACTIONS IN THE PILOT SCALE AIR TREATMENT SYSTEM

The photolytic reactors in the pilot scale system have been modified based on results from the analytical and bench scale studies. The pilot scale treatment system contains two photolytic reactors labeled as the ambient humidity and high humidity photolytic reactors, respectively, in Figure 1. The first reactor is operated at ambient humidity conditions, and the second is operated at approximately 100% relative humidity after the air stream has first passed through the chemical absorption reactors. The photolytic reactors within the pilot scale system utilize approximately 120 ppm ozone in a 20 cfm exhaust from the water recycle tank. Up to seven bulbs spaced 12 inches apart were used in the photolytic reactors in the pilot scale system. The bulbs were 40 W low pressure mercury vapor lamps, which have approximately 90% of their light output centered at 254 nm.

Several pilot scale experiments were conducted for 2 to 12 hours. One run with ethanol, one with ethylbenzene, three with MEK, and two with trichloroethylene (TCE) provided information on photolytic reactivity in the system. Data for each solvent, and data at two system flow rates and with 3 and 7 UV bulbs has been analyzed.

The runs with ethanol and ethylbenzene showed no detectable degradation of either compound within the photolytic reactors. The inlet and outlet air concentrations of ethanol and ethylbenzene were within the experimental error of the analytical method (Relative Standard Deviation [RSD] 5%). Furthermore, no additional peaks from possible degradation products were detected. These results are not surprising since neither ethanol or ethylbenzene is a strong absorber of UV radiation.

Around the photolytic reactors the influent and outlet concentrations of MEK, as with ethanol and ethylbenzene, were within the experimental error. A possible degradation product of MEK was observed at the outlet of the photolytic reactor with cryogenically concentrated GC/FID analysis, but this byproduct could not be identified by the GC/MS method available. The byproduct peak was not detected at flow rates of 2600 cfm with only three bulbs operating. With seven bulbs operating at a flow rate of 2600 cfm, the possible byproduct peak from GC/FID analysis had a response of 0.4% of the MEK response. At flow rates of 1300 cfm, the response of the potential by-product peak doubled to 0.8% of the MEK response. Thus the presence of the by-product peak seems to agree with prediction of

the analytical model, that increased residence times within the reactor and increased light intensity increases photolytic degradation.

Trichloroethylene (TCE) was significantly degraded in the photolytic reactors. TCE , like many halocarbons is very reactive with UV radiation [15,16]. The percent of TCE degraded in each photolytic reactor for each run is shown in Figure 7. When the pilot scale APCS was operated at 2600 cfm with seven bulbs on, the average TCE degradation in each photolytic reactor was 30% of the influent concentration into each reactor. When the flow rate was reduced to 1300 cfm, the average degradation increased to 46% in the first reactor and 48% of the influent concentration into each reactor in the second reactor. This agrees with the qualitative model predictions of increased degradation with increased residence times.

No byproducts were detected in the GC/ECD analysis of any air phase TCE sample. However, the pH of the water in the chemical absorption unit dropped form a pH of 6 to 2 in fifteen minutes. It is proposed that the degradation of TCE lead to the formation of hydrochloric acid (HCl) via the following pathway:

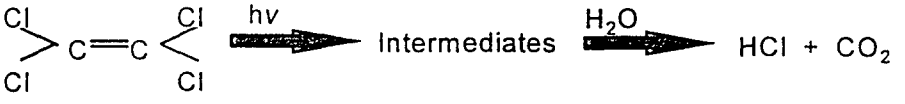

It appears from the rapid drop from pH 7 to pH 2.8 of the scrubbing liquid, that the HCl was absorbed in the chemical absorption reactors.

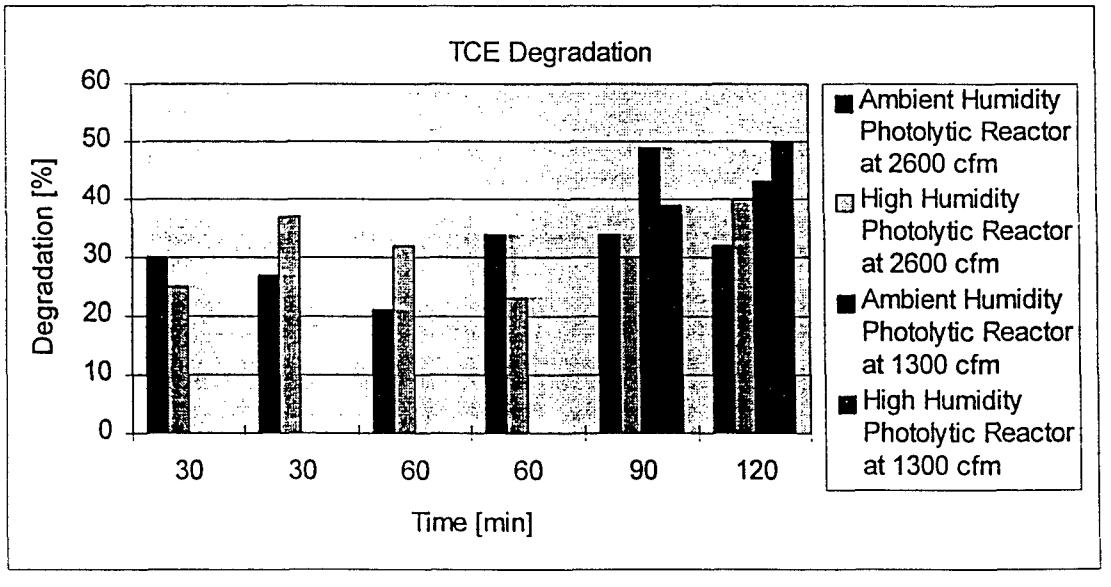

Figure 7: TCE Degradation in the pilot scale photolytic reactors (These values represent the percent degradation of the concentration entering each reactor.)

The data from the pilot scale photolytic reactors is summarized in Table II. As expected, organic compounds which are poor absorbers of UV radiation were not

significantly degraded in the pilot scale system. However, a twenty to fifty percent decrease of TCE, a good absorber of UV radiation, was observed in each photolytic reactor. Analytical predictions were confirmed through bench and pilot scale experimentation. Increased light intensity, increased residence time and increased ozone concentration within a photolytic reactor all increased organic destruction efficiencies.

TABLE II - EFFECTS OF THE PILOT SCALE PHOTOLYTIC REACTOR

Solvent	Effects of the Pilot-scale Photolytic Reactor
Ethanol	No measurable effect
Ethylbenzene	No measurable effect
Methyl ethyl ketone	0.5 % Byproduct formation
Trichloroethylene	20-50% decrease in TCE; Formed hydrochloric acid

PILOT SCALE AQUEOUS PHASE ABSORPTION

The original pilot scale system consisted of two packed column chemical absorption reactors in series which facilitated the mass transfer of VOCs into the aqueous phase. The cross-sectional area of the packed columns was 6.67 ft^2, and the height of the packing in each column was 8 ft. The packing used in the column was 3" diameter random packed plastic media. The water flow through the column was 100 gal/min flowing countercurrent to the 2600 cfm air stream. The scrubbing liquor from each reactor was pumped to separate water recycle tanks and ozonated with 150 ppm ozone in a 20 cfm air stream. The water had a ten minute retention time in the water recycle tank before being recirculated through the chemical absorption reactors. The absorption of VOCs in the water was found to be highly dependent upon the vapor pressure and water solubility of the particular VOC, as well as a function of the concentration of the VOC in the scrubbing liquor.

Ethanol is a highly polar organic compound which is totally miscible in water. Ethanol was readily absorbed in the pilot scale packed column because of its high solubility and relatively low vapor pressure. About 90% of the ethanol was absorbed in each reactor during the first thirty minutes of each run, resulting in a total removal efficiency of approximately 99%. However, the removal efficiency of each reactor decreased over time as the ethanol concentration in the water increased.

After six hours of spraying ethanol into the inlet of the pilot scale system, only 45% of the ethanol was removed in the first reactor, and only 68% of the remaining ethanol was removed in the second reactor. Thus, the overall removal efficiency of ethanol in the pilot scale packed column chemical-absorption reactors was reduced to 82%. After six hours of operation, the experiment was discontinued; however, it is expected that the removal efficiency would continue to decrease until equilibrium between the air and water phase is reached.

Methylethyl ketone (MEK) is a semi-polar compound with a solubility of 353 g/l in water at 10° C. Due to its limited solubility in water, the decrease in the removal efficiency of MEK in the absorption reactors was more rapid than for ethanol. After five minutes of

operation the removal efficiency of MEK in the first reactor was 76% and the combined removal efficiency of both reactors was 92%. However after one hour of operation the removal efficiency of the first reactor had dropped to 26%, and the combined removal efficiency had dropped to 57%. After two hours of operation, MEK was no longer removed by the chemical absorption reactors.

Ethylbenzene has a very limited solubility in water (152 mg/l). The removal efficiency of the packed column chemical absorption reactors dropped rapidly because of this limited solubility. After only five minutes of operation, the ethylbenzene concentration had reached its maximum solubility in the water, and no more ethylbenzene was removed from the air stream by the chemical absorption reactors.

Trichloroethylene reacted differently in the chemical absorption reactors than the other solvents. There was no significant removal of TCE in the second chemical-absorption reactor. Since TCE has the lowest solubility of the four solvents tested, this was expected. However, an average of 23% of the TCE was removed in the first reactor throughout the entire time TCE was being sprayed into the pilot scale system. It is proposed that the degradation of TCE which occurred in the first chemical absorption reactor was caused by TCE reactions with intermediates formed in the upstream photolytic reactor.

The data from the pilot scale chemical absorption reactors is summarized in Table III. Ethanol, a polar compound, was readily absorbed into the water as expected. The removal efficiency was much lower for less polar compounds. Ozonation alone did not significantly decrease the concentration of the organics in the scrubbing liquor. Consequently the removal efficiency of the chemical absorption reactors decreased over time. Thus, subsequent bench scale studies were conducted to enhance chemical oxidation of VOCs transferred to the aqueous phase as discussed below.

Less polar compounds reached their maximum solubility more quickly than polar compounds. This data is consistent with Henry's Law which governs mass transfer. Destruction of the organic in the scrubbing liquor is critical to achieve continuous removal and destruction in the pilot scale chemical-absorption reactors. This is especially critical for semi-polar compounds such as MEK which may be effectively removed by absorption processes, but only if chemical reactions occur fast enough to keep the MEK concentration in the scrubbing liquor low.

TABLE III - MAXIMUM SOLVENT CONCENTRATION IN THE WATER DURING THE PILOT SCALE TESTS

Solvent	Maximum Concentration Achieved in the Water	Time at which the Maximum Concentration Occurred
Ethanol	610 mg/l and still increasing	6 hours
Methylethyl ketone	120 mg/l	2 hours
Ethylbenzene	4 mg/l	1 minute
Trichloroethylene	6 mg/l	1 minute

RESULTS OF BENCH SCALE AQUEOUS PHASE EXPERIMENTS

In light of these initial pilot scale tests, the authors sought a more effective chemical oxidation process. Specifically, advanced oxidation processes were studied to improve aqueous phase destruction of the organic solvents, because destruction is critical to the removal efficiency of the chemical absorption reactors in the pilot scale system. The MCLB has approved a new surface coating which uses NMP as a solvent. There was no literature which described NMP reactions in AOP processes, so the degradation and optimization of NMP in a CSTR was studied. The effects of pH variations, ozone dose rate, and hydrogen peroxide concentration were determined in a full factorial design study.

The full factorial design allowed direct comparison between the effect each variable has upon the system and any interactions between the variables. Increasing the pH from 7 to 9 produced the greatest increase upon the reaction rate, improving it by 130%. Increasing the ozone dose rate from 3.1 mg/min to 6.2 mg/min in the diffused air stream also increased the reaction rate by 65%. However increasing the rate of hydrogen peroxide addition from to 5.6 mg/min to 11.2 mg/min did not increase the reaction rate. No reaction rate increase was seen with hydrogen peroxide increases when the hydrogen peroxide to ozone ratio in the water exceeded 3.5. These effects are summarized in Table IV, and are consistent with the results of Glaze *et al.*[17].

Staehelin and Hoigne predicted there were synergistic effects between ozone, hydrogen peroxide and pH in oxidation reactions [18]. The effects of these interactions was examined in the full-factorial set of experiments which were conducted. The interaction effects were determined by comparing the degradation of NMP when two of the variables were at the extreme conditions (high-high and low-low) and when the same two variables were at non-extreme conditions (high-low and low-high). The overall effect of the interaction is judged by the magnitude of the difference in the degradation rate of NMP.

TABLE IV - MAIN VARIABLE EFFECTS UPON THE DEGRADATION RATE OF NMP

Variable	High Value	Low Value	Change in the Reaction Rate %
pH	9	7	+130%
Ozone addition (Gas Phase)	6.2 mg/min	3.1 mg/min	+65%
Hydrogen peroxide addition	11.2 mg/min	5.6 mg/min	-8%

The NMP degradation rate increased by a factor of 1.29 due solely to the interactions of ozone and pH. This effect was in agreement with the literature that has suggested ozone is decomposed more rapidly at higher pH levels. The ozone and hydrogen peroxide interactions increased the degradation rate of NMP by 15%. The interactions of hydrogen peroxide and pH were within experimental error (RSD 8%) and did not significantly effect the degradation rate of NMP. Table V summarizes the effects of these interactions.

TABLE V -VARIABLE INTERACTION EFFECTS UPON THE DEGRADATION RATE OF NMP: COMPARISON OF HIGH-HIGH VERSUS LOW-LOW VALUES OF THE VARIABLE INTERACTIONS

Variable Interactions	Change in the Reaction Rate [g/l-hr]
Ozone & pH	30%
Ozone & Hydrogen Peroxide	15%
Hydrogen Peroxide & pH	7%

The result of the full factorial design experiments indicated that increasing the pH and ozone dose rate enhanced the destruction of NMP. Experiments were conducted at pH 9 and the maximum ozone dose rate of 6.2 mg/min to determine the optimum molar ratio of hydrogen peroxide to ozone. The optimum ratio shown in Figure 8 was approximately 0.5 moles of hydrogen peroxide per mole of ozone which is in agreement with the stoichiometry predicted by Staehelin and Hoigne [18]. A slight decrease in the reaction rate when excess hydrogen peroxide is present was observed, in agreement with Glaze *et al.* [18]. Glaze *et al.* suggested this may be due to hydrogen peroxide scavenging of the hydroxyl radicals.

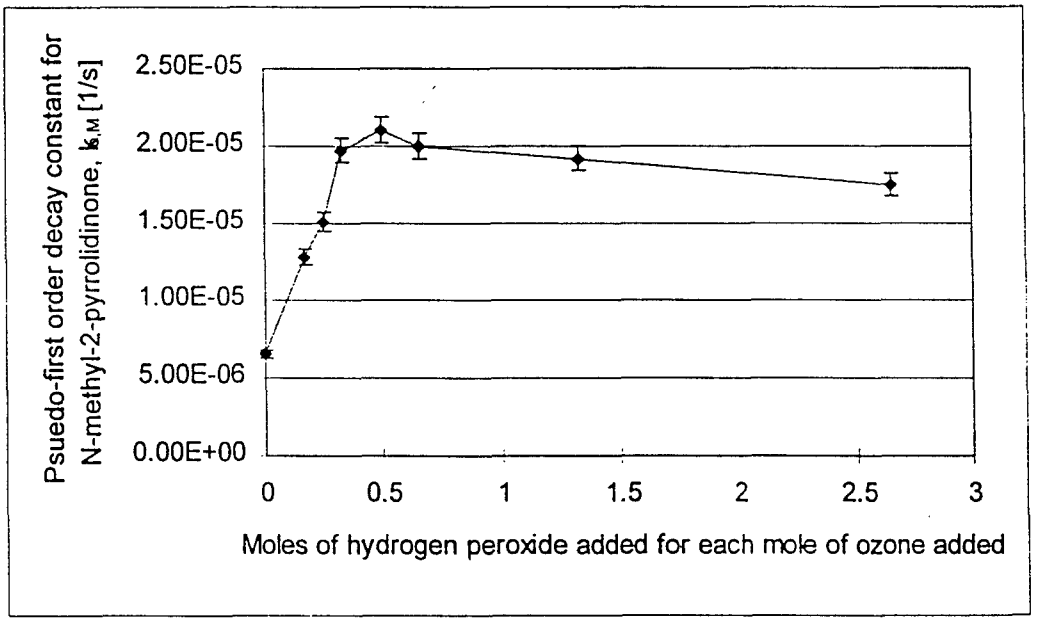

Figure 8: Optimization of the hydrogen peroxide addition rate

PILOT SCALE MODIFICATION OF THE CHEMICAL ABSORPTION REACTORS

The literature cited and the bench scale aqueous phase experiments indicate that hydrogen peroxide addition to ozone treatment may significantly increase the destruction of

many organics in the aqueous phase. The reaction rates can be increased in pure water by increasing the pH, the ozone dose rate, and maintaining a molar ratio of 0.5 mole of hydrogen peroxide per mole of ozone in the aqueous solution. Modifications were made to the first pilot scale chemical absorption reactor by adding 0.1 ml/min of hydrogen peroxide to maintain the optimum molar ratio of 0.5 moles of hydrogen peroxide per mole of ozone, and adding sodium hydroxide to maintain a pH of 8.3.

The removal efficiency of MEK from the air stream in the modified pilot scale chemical absorption reactors was determined. The solvent MEK was chosen because it exhibited the greatest change in the removal efficiency over a two hour time period, with 92% removal after 5 minutes of operation, and no measurable removal after two hours of operation as shown in Figure 9. The effects of hydrogen peroxide addition and pH control to the first chemical absorption reactor upon the combined removal efficiency of MEK in the chemical absorption reactors are summarized in Table VI. After one hour, the removal efficiency of the modified chemical absorption reactors was increased by more than 40% over the removal efficiency without hydrogen peroxide addition and pH control. MEK was removed in the modified system for more than 5 hours, whereas no MEK was removed past two hours prior to hydrogen peroxide addition.

Variations of approximately 10% in the removal efficiency shown in Figure 9 were caused by fluctuation in the inlet concentration. Variations in the inlet concentration cause changes in the driving force which influence the mass transfer in the reactor. These fluctuations combined with the standard deviations in the analytical method explain why negative removal efficiencies and fluctuations occur after the water had been saturated with MEK during ozone treatment.

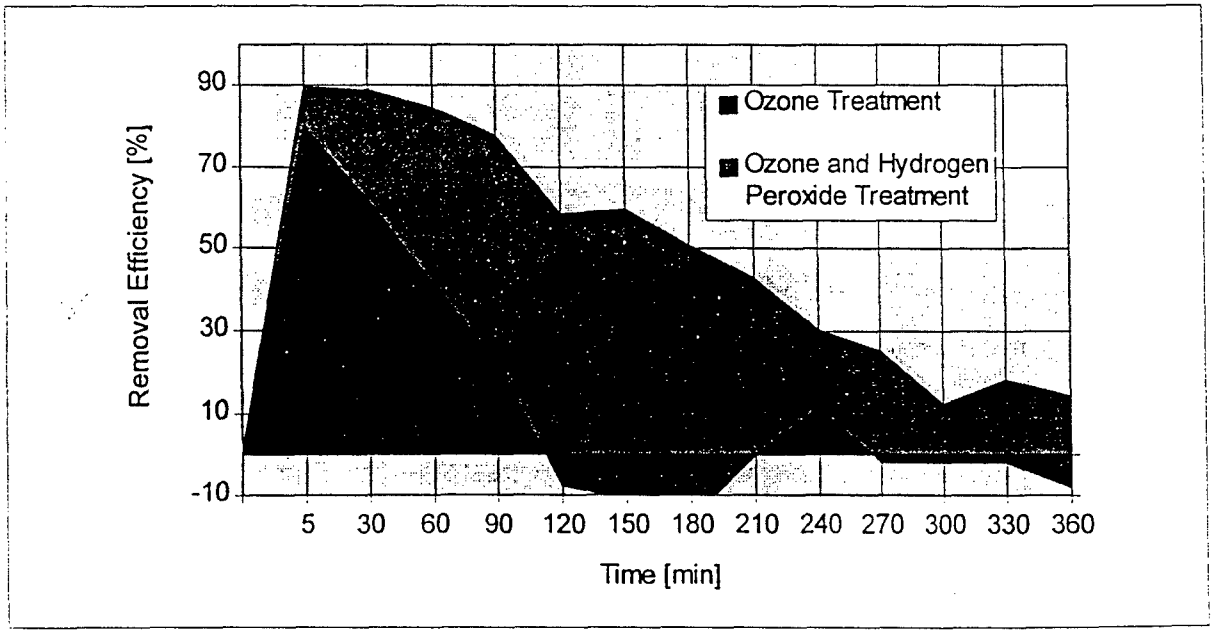

Figure 9: Effects of pH control and hydrogen peroxide addition on the removal efficiency of MEK in the pilot scale chemical absorption reactors

TABLE VI - EFFECTS OF pH CONTROL AND HYDROGEN PEROXIDE ADDITION ON THE REMOVAL EFFICIENCY OF MEK IN THE PILOT SCALE CHEMICAL ABSORPTION REACTORS

Time (min)	Removal Efficiency (%)	
	Ozone Addition	Ozone and Hydrogen Peroxide Addition
5	80	90
60	61	89
120	-8	58
240	11	30
360	-8	14

The increase in the removal efficiency by pH control and hydrogen peroxide addition to the chemical absorption reactors was significant. However, the reaction rates were still insufficient to maintain a removal efficiency greater than 30% of the concentration entering the reactors past five hours of operation in the chemical absorption reactors. Thus, the ozone dose rate, pH or the retention time in the water recycle tanks should be increased to achieve continuous removal.

ANALYSIS OF REGENERATED CARBON IN OPERATIONAL FULL-SCALE SYSTEMS

In the full scale systems, the granular activated carbon undergoes daily cycles of VOC loading and activated oxygen regeneration. Ozone and other radicals are produced in high pressure UV/ozone generators and introduced into the carbon beds. Theoretically, the GAC serves as a type of "capacitor" for the adsorbed VOCs, which allows long retention times within the treatment system for the ozone and UV generated radicals to oxidize the VOCs.

Singh, 1995 evaluated the GAC employed in VOC laden air treatment systems from (a) an aircraft panel manufacturer, (b) a furniture coating manufacturer, and (c) an aircraft coating manufacturer [3,19]. Virgin sample of the GAC from (a) and (b) were also evaluated.

The adsorption capacity of the GAC for the virgin samples and regenerated samples have been compared and the results are shown in Table VII. Also, a qualitative comparison is shown for the regenerated GAC from (c) and a formulated virgin sample that is believed to have properties similar to a virgin sample from (c). It was observed that the GAC from (a) following one year of service and 400-800 regenerative cycles lost 17% to 35% of its virgin adsorption capacity for the solvents tested under the analytical conditions that were employed. Similarly, the GAC from (b) lost 23%-58% of its adsorption capacity following 2½ years of service or 1000-2000 regenerations. In contrast, it is expected that GAC would have been completely destroyed if it had been exposed to the same number of thermal oxidation regenerations.

The regenerated carbon exhibited a greater reduction in adsorptive capacity for polar compounds than for non-polar compounds. This is a useful observation when applied to the

hybrid treatment system. For example, the GAC from the furniture manufacturer exhibited a 55% reduction in its adsorptive capacity of ethanol. The reduction of the capacity in the GAC for aromatic non-polar compounds from the furniture manufacturer was only 23% to 34%. The adsorptive capacity of the GAC for PCE, a chlorinated compound, and MIBK, a semi-polar compound, was moderately reduced, 36% and 43% respectively.

However, in the pilot scale system, most of the ethanol was removed in the chemical-absorption reactors. Since similar aromatic non-polar compounds were not removed in either the photolytic reactors or the chemical-absorption reactors, it is most important that the carbon bed be able to adsorb aromatic non-polar compounds. Moderate reduction in the GAC capacity for semi-polar and chlorinated compounds is acceptable since chlorinated compounds are destroyed in the photolytic reactors, and semi-polar compounds can be removed to a large extent in the modified chemical-absorption rectors.

TABLE VII - ADSORPTION CAPACITY OF VIRGIN AND REGENERATED GAC USED IN FULL-SCALE OPERATING AIR TREATMENT SYSTEMS [3]

Sample	Methanol (mg/ml)	Ethanol (mg/ml)	MIBK (mg/ml)	Benzene (mg/ml)	Toluene (mg/ml)	PCE (mg/ml)
Virgin Aircraft Panels	202	176	146	196	181	269
Regenerated Aircraft Panels	137	128	95	163	134	210
% Reduction	32%	27%	35%	17%	26%	22%
Virgin Furniture Coating	154	143	117	167	151	223
Regenerated Furniture Coating	65	65	65	128	99	142
% Reduction	58%	55%	43%	23%	34%	36%
Formulated Virgin	189	171	136	192	172	253
Regenerated Aircraft Coating	128	128	108	143	134	198
% Reduction	32%	25%	20%	25%	22%	22%

SUMMARY OF THE PILOT SCALE RESULTS

As discussed above, pilot scale testes evaluated the effectiveness of a 2600 cfm hybrid system shown in Figure 1. VOC concentrations were monitored at the inlet and outlet of the individual reaction units, the ambient humidity photolytic reactor, each of the chemical absorption reactors, the high humidity photolytic reactor, and the main granular activated carbon (GAC) adsorption bed. These tests measured the removal achieved for ethanol, methylethyl ketone (MEK), trichloroethylene (TCE), and ethylbenzene as shown in Figures 10-14. None of these tests employed hydrogen peroxide enhancement or pH

adjustment, with the exception of one MEK test (Figure 12). The GAC bed received no advanced oxidation regeneration during these experiments, and the initial virgin GAC capacity for adsorbing these VOCs did not appear to be exceeded during the 100 hours of operation.

Concentration profiles were developed from the pilot scale tests and are shown in Figures 10 through 14. These profiles indicate what part of the hybrid system is most important for treating different classes of VOCs.

Ethanol, a very polar compound, was largely removed in the chemical absorption reactors over six hours as shown in Figure 10. The photolytic reactors did not significantly reduce the ethanol concentrations in the air stream. The remainder of the ethanol which was not absorbed into the ozonated water was adsorbed onto the virgin carbon beds in the pilot scale system. Thus from the pilot scale data and evaluation of GAC from operating systems, the chemical absorption reactors may be the best removal mechanism for polar compounds.

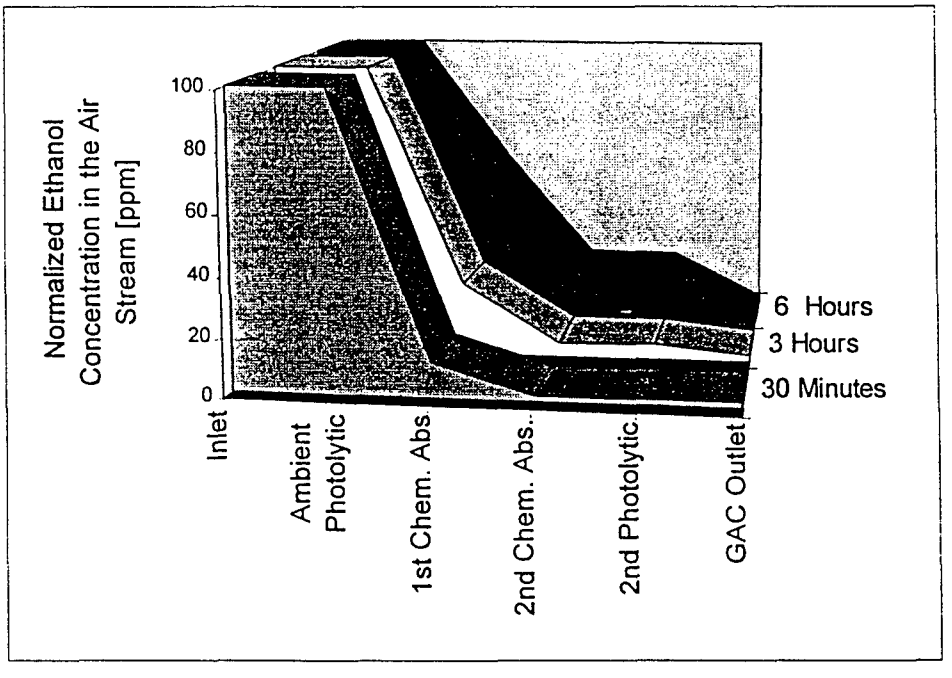

Figure 10: Ethanol concentration profile in the pilot scale system

Methylethyl ketone (MEK) is a semi-polar compound. The photolytic reactors appear to start the degradation process of MEK. MEK was also removed in the chemical absorption reactors as shown in Figure 11. Without degradation of MEK in the aqueous phase, equilibrium was rapidly established. And, after two hours of operation without the addition of pH control, or hydrogen peroxide, GAC was the only significant removal mechanism for MEK.

However, with the addition of pH control and hydrogen peroxide, significant removal occurred in the chemical absorption reactors up to six hours as shown in Figure 12. Thus, when the concentration of MEK in the aqueous phase can be reduced by advanced oxidation processes, the chemical absorption reactors and the GAC both significantly reduced the concentration of MEK from the exhaust air stream.

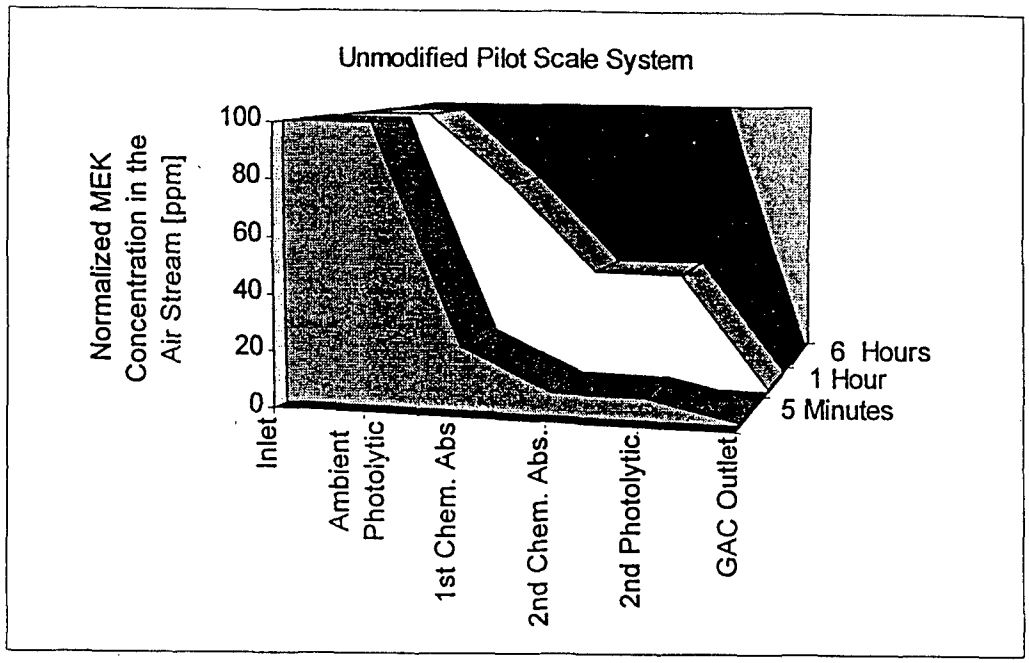

Figure 11: MEK concentration profile in the pilot scale system without pH control or hydrogen peroxide addition.

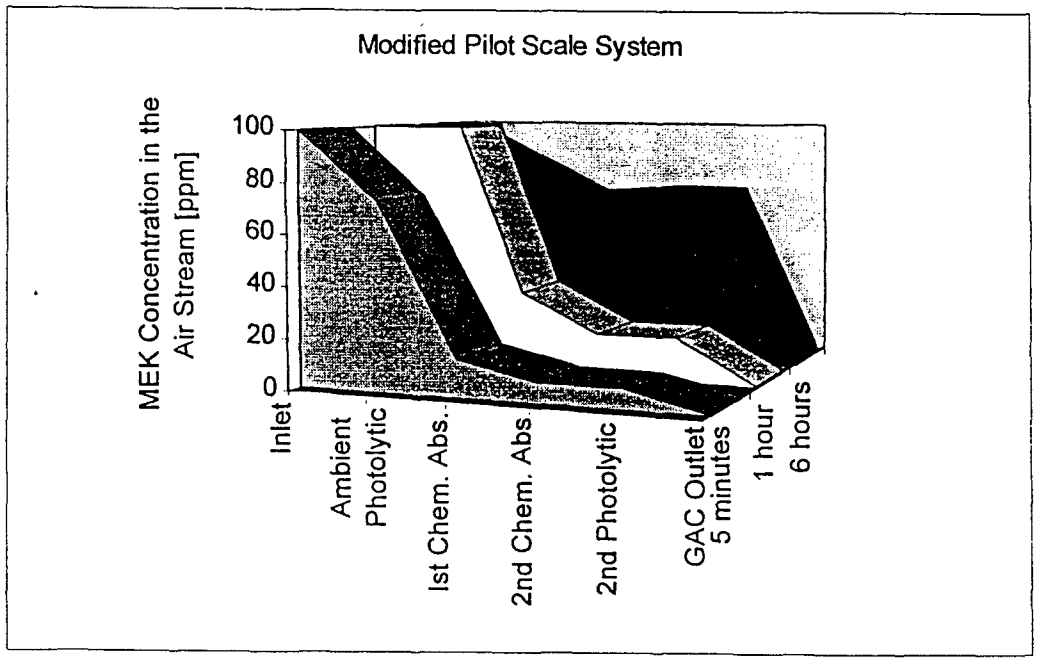

Figure 12: MEK concentration profile in the pilot scale system with pH control and hydrogen peroxide addition.

Trichloroethylene was significantly removed in the photolytic reactors as shown in Figure 13. The destruction of TCE continued into the first chemical-absorption unit. Based upon the pilot scale data, placing the photolytic reactors upstream of the chemical absorption reactors may be beneficial. The photolytic reactors and the chemical absorption reactors in combination removed a large fraction of the chlorinated VOC before the virgin GAC bed. The hybrid system with virgin GAC removed over 90% of the TCE from the air stream.

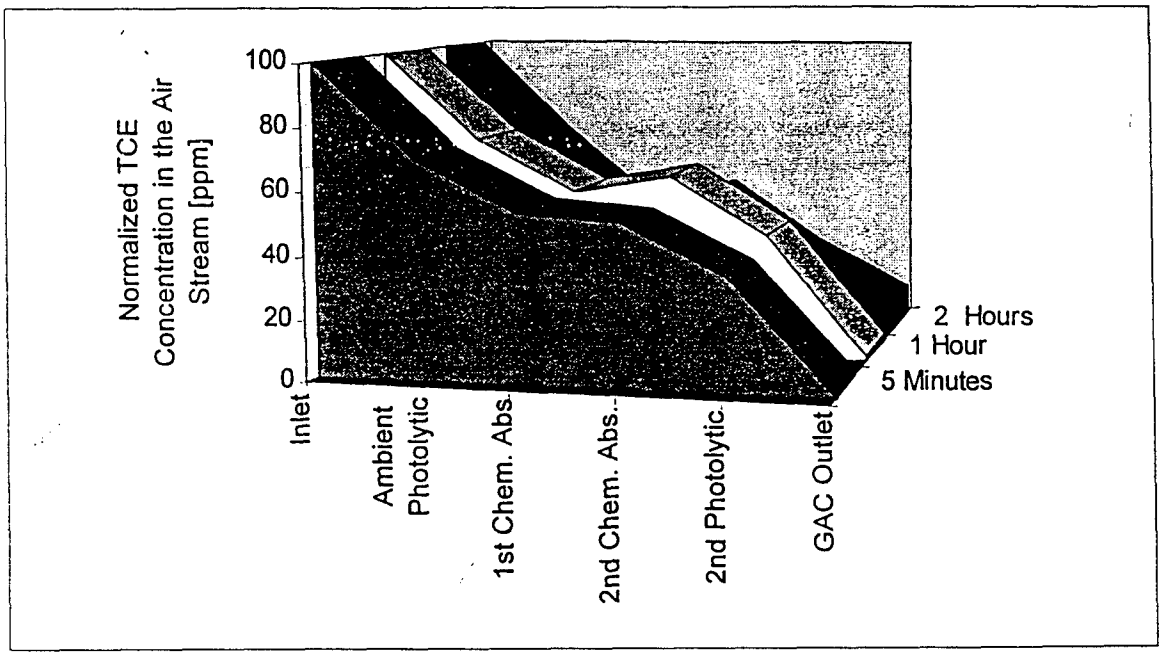

Figure 13: TCE concentration profile in the pilot scale system

The concentration profile of ethylbenzene, an aromatic compound, throughout the pilot scale system is shown in Figure 14. Ethylbenzene in the pilot scale system was removed primarily in the virgin GAC.

In comparison to these results, the evaluations of regenerated GAC described above from full scale operational treatment systems suggested that UV/ozone regenerated GAC retained more capacity to remove non-polar compounds than polar compounds. The GAC retained part of its original adsorptive capacity after several years of service. Thus from the pilot scale data and evaluation of GAC from operating systems, the regenerative carbon adsorption beds may be best suited for removing non-polar compounds.

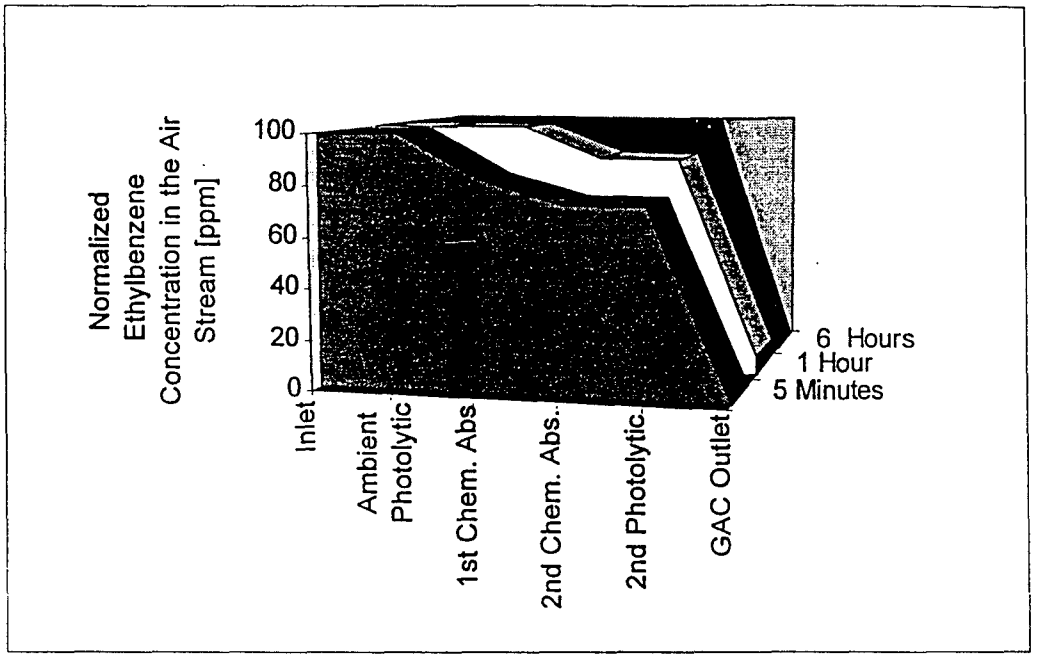

Figure 14: Ethylbenzene concentration profile in the pilot scale system

CONCLUSIONS

Advanced oxidation processes have an important role in innovative VOC treatment systems. It has been demonstrated that the photolytic reactors, chemical absorption reactors and the virgin GAC in the pilot scale treatment system are capable of removing a large variety of VOCs from an exhaust air stream.

Each solvent behave differently in the hybrid system as shown above in Figures 10 to 14. Polar compounds with high water solubilities are removed predominantly in the chemical absorption reactors. Chlorinated solvents that are highly photoreactive are destroyed due to chemical reactions initiated in the photolytic reactors. Semi-polar compounds may be removed through a combination of absorption and advanced oxidation reactions along with adsorption onto GAC. Non-polar compounds may be continuously removed by GAC absorption and regeneration by advanced oxidation processes. Thus, when an air stream is composed of mixed or varying solvent concentrations, each solvent will be removed and destroyed by a combination of technologies uniquely suited to its physical and chemical characteristics.

Thermal oxidizers require significant fuel costs to maintain destruction efficiencies when relatively low concentrations (<1000 ppm) are present in the exhaust air stream. Pure absorption air treatment processes are limited to low flow rates and polar compounds only. Disposal of spent activated carbon requires continual replacement and the risk of rapidly rising disposal costs. Therefore, hybrid air treatment systems which use advanced oxidation technology are a promising treatment alternative for low concentration, variable composition and high volumetric flow rate exhaust air streams.

Design of future pilot scale systems should take into consideration the types of solvents to be treated and their relative concentrations. Incorporating more UV lights at closer intervals, increasing the ozone concentration throughout the system, adding hydrogen peroxide to the water and controlling the pH of the water may result in a more effective air pollution control system design.

REFERENCES

1. Seinfeld, J. H. 1986. Atmospheric chemistry and physics of air pollution, New York, NY: John Wiley & Sons, Inc., pp. 42.

2. Mallery, M. 1995. Numerical Model of Formaldehyde Photo-oxidation in a Two-Dimensional Flow Field Over Cylindrical UV Light Sources, A Thesis in Mechanical Engineering, The Pennsylvania State University, State College, PA.

3. Singh, J. and F. S. Cannon. 1995. "Characterization of Advanced Oxidation Regenerated GAC's," in Innovative Technologies for Site Remediation and Hazardous Waste Management; Proceedings of the National Conference, American Society of Civil Engineers, New York, NY, pp. 449-456.

4. Cannon, F. S., J. S. Dusenbury, P. D. Paulsen, J. Singh, D. Mazyck, and D. Maurer, "Advanced Oxidant Regeneration of Granular Activated Carbon for Controlling Air-Phase VOCs." in press, Ozone Science and Engineering, (1996).

5. Barker, R. and A. R. Jones, 1988. "Treatment of malodorants in air by the UV/ozone technique." Ozone Science and Engineering. 10:405-418.

6. Ayer, J. and D. Urry, 1994. "Spray Booth Emission Control System Demonstration Project, Phase I Interim Report: Pre-Modification Baseline and Continuation Studies," Acurex Environmental Corporation, Irvine, CA.

7. Albano, M. 1994. Computer Simulation of a Photolytic Reactor to Study the Effects of a Variety of Wavelengths, A Thesis in Environmental Pollution Control, The Pennsylvania State University, State College, PA.

8. Schmelzle, J. P. 1994. Ultraviolet Photochemical and Radical Oxidation of Airborne Volatile Organic Compounds, A Thesis in Environmental Pollution Control, The Pennsylvania State University, State College, PA.

9. DeMore, W. B., S. P. Sander, D. M. Golden, R. F. Hampson, M. J. Kurylo, C. J. Howard, A. R. Ravishankara, C. E. Kolb, and M. J. Molina. 1992. "Chemical Kinetics and Photochemical Data for Use in Stratospheric Modeling," JPL Publication 92-20.

10. Anatasi, C., R. V. Gladstone, and M. G. Sanderson, 1993. "Chemical Amplifiers for Detection of Peroxy Radicals in the Atmosphere" Environmental Sci. Technol, 27(3): 474-482.

11. Atkinson, R., D. L. Baulch, R. A. Cox, R. F. Hampson, J. A. Kerr, and J. Troe, 1992. "Kinetic and Photochemical Data for Atmospheric Chemistry Supplement IV." J. Phys. Chem. Ref. Data, 21:1125-1173.

12. Calvert, J. G., and J.N. Pitts. 1966. Photochemistry, New York, NY: John Wiley & Sons, Inc.

13. Hoigne, J., and H. Bader, 1976. "The role of hydroxyl radical reactions in ozonation processes in aqueous solutions." Water Research, 10:377-386.

14. Hoigne, J., and H. Bader, 1979. "Ozonation of water: Selectivity and Rate of oxidation of solutes." Ozone: Science and Engineering, 1:73-85.

15. Sanhueza, E., I. C. Hisatsune, and J. Heicklen, 1976. "Oxidation of Haloethylenes." Chemical Reviews, 76(6):801-826.

16. Heltz, G. R., R. G. Zepp, and D. G. Crosby. 1994. Aquatic and Surface Photochemistry, Boca Raton, FL: Lewis Publishers, pp. 484-528.

17. Glaze, W. H., J. Kang, and D. H. Chapin, 1987. "The Chemistry of Water Treatment Processes Involving Ozone, Hydrogen Peroxide and Ultraviolet Radiation." Ozone Science and Engineering, 9:335-352.

18. Staehelin, J., and J. Hoigné, 1982. "Decomposition of Ozone in Water: Rate of Initiation by Hydroxide Ions and Hydrogen Peroxide." Environmental Science and Technology, 16:676-681.

19. Singh, J. 1995. Reactivation of Air-Phase GAC Using Advanced Oxidation. A Thesis in Environmental Engineering, The Pennsylvania State University, State College, PA.

NOMENCLATURE

C	Species Concentration	U	Gas Velocity
D	Molecular Diffusion Coefficient	μ_T	Turbulent Viscosity
I_{ro}	Light Intensity bulb Surface	ϕ	Quantum Yield
$J(\lambda)$	Actinic Flux	ρ	Gas Density
r	Distance from bulb	σ	Absorp. Cross-Sect.
r_o	Bulb radius	σ_s	Turbulent Prandtl No.